

# Generation of paired photons in a quantum separable state in Bragg reflection waveguides

Jiří Svozilik<sup>1,2</sup>, Martin Hendrych<sup>1</sup>, Amr S. Helmy<sup>3</sup>, and Juan P. Torres<sup>1,4</sup>

<sup>1</sup> ICFO-Institut de Ciències Fòtiques, Mediterranean Technology Park, 08860 Castelldefels (Barcelona), Spain

<sup>2</sup> Joint Laboratory of Optics, Palacký University and Institute of Physics of Academy of Science of the Czech Republic, 17. listopadu 50A, 772 07 Olomouc, Czech Republic

<sup>3</sup> Edward S. Rodgers Department of Electrical and Computer Engineering, University of Toronto, 10 King's College Road, Toronto, Ontario M5S3G4, Canada

<sup>4</sup> Departament of Signal Theory and Communications, Universitat Politècnica de Catalunya, 08034 Barcelona, Spain

**Abstract:** This work proposes and analyses a novel approach for the generation of separable (quantum uncorrelated) photon pairs based on spontaneous parametric down-conversion in Bragg reflection waveguides composed of semiconductor AlGaIn layers. This platform allows the removal of any spectral correlation between paired photons that propagate in different spatial modes. The photons can be designed to show equal or different spectra by tuning the structural parameters and hence the dispersion of the waveguide.

© 2018 Optical Society of America

**OCIS codes:** (190.4410) Nonlinear optics, parametric processes; (270.0270) Quantum optics

[jiri.svozilik@icfo.es](mailto:jiri.svozilik@icfo.es)

## References and links

1. P. P. Rohde, G. J. Pryde, J. L. O'Brien, and T. C. Ralph, "Quantum gate characterization in an extended Hilbert space", *Phys. Rev. A* **72**, 032306 (2005).
2. I. A. Walmsley, and M. G. Raymer, "Toward Quantum-Information Processing with Photons", *Science* **307**, 1733 (2005).
3. P. Kok, W. J. Munro, K. Nemoto, T. C. Ralph, J. P. Dowling, and G. J. Milburn, "Linear optical quantum computing", *Rev. Mod. Phys.* **79**, 135 (2007).
4. L. E. Vicent, A. B. U'Ren, R. Rangarajan, C. I. Osorio, J. P. Torres, L. Zhang, and I. A. Walmsley, "Design of bright, fiber-coupled and fully factorable photon pair sources", *New J. Phys.* **12**, 093027 (2010).
5. T. Aichele, A. I. Lvovsky, and S. Schiller, "Optical mode characterization of single photons prepared by means of conditional measurements on a biphoton state", *Eur. Phys. J. D* **18**, 237 (2002).
6. W. P. Grice, A. B. U'Ren, and I. A. Walmsley, "Eliminating frequency and space-time correlation in multiphoton states", *Phys. Rev. A* **64**, 063815 (2001).
7. P. J. Mosley, J. S. Lundeen, B. J. Smith, P. Wasylczyk, A. B. U'Ren, C. Silberhorn, and I. A. Walmsley, "Heralded generation of ultrafast single photons in pure quantum states", *Phys. Rev. Lett.* **100**, 133601 (2008).
8. J. P. Torres, F. Macià, S. Carrasco, and L. Torner, "Engineering the frequency correlations of entangled two-photon states by achromatic phase matching", *Opt. Lett.* **30**, 314 (2005).
9. M. Hendrych, M. Mičuda, and J. P. Torres, "Tunable control of the frequency correlations of entangled photons", *Opt. Lett.* **32**, 2339 (2007).

10. J. P. Torres, M. Hendrych, and A. Valencia, "Angular dispersion: an enabling tool in nonlinear and quantum optics", *Adv. Opt. Photon.* **2**, 319 (2010).
11. Z. D. Walton, M. C. Booth, A. V. Sergienko, B. E. A. Saleh, and M. C. Teich, "Controllable frequency entanglement via auto-phase-matched spontaneous parametric down-conversion", *Phys. Rev. A* **67**, 053810 (2003).
12. A.B. U'Ren, K. Banaszek, and I.A. Walmsley, "Photon engineering for quantum information processing", *Quantum Inf. Comput.* **3**, 480 (2003).
13. S. Carrasco, J. P. Torres, L. Torner, A. V. Sergienko, B. E. Saleh, and M. C. Teich, "Spatial-to-spectral mapping in spontaneous parametric down-conversion", *Phys. Rev. A* **70**, 043817 (2004).
14. A. Valencia, A. Ceré, X. Shi, G. Molina-Terriza, and J. P. Torres, "Shaping the waveform of entangled photons", *Phys. Rev. Lett.* **99**, 243601 (2007).
15. X. Shi, A. Valencia, M. Hendrych, and J. Torres, "Generation of indistinguishable and pure heralded single photons with tunable bandwidth", *Opt. Lett.* **33**, 875 (2008).
16. A. B. U'Ren, R. K. Erdmann, M. de la Cruz-Gutierrez, and I. A. Walmsley, "Generation of Two-Photon States with an Arbitrary Degree of Entanglement Via Nonlinear Crystal Superlattices", *Phys. Rev. Lett.* **97**, 223602 (2006).
17. B. R. West and A. S. Helmy, "Dispersion tailoring of the quarter-wave Bragg reflection waveguide", *Opt. Express* **14**, 4073 (2006).
18. P. Abolghasem, M. Hendrych, X. Shi, J. P. Torres, and A. Helmy, "Bandwidth control of paired photons generated in monolithic Bragg reflection waveguides", *Opt. Letters* **34**, 2000 (2009).
19. J. Jin, *The Finite Element Method in Electromagnetics, 2nd Edition*, (Wiley-IEEE Press, 2002).
20. G. M. Laws, E. C. Larkins, I. Harrison, C. Molloy, and D. Somerford, "Improved refractive index formulas for the  $\text{Al}_x\text{Ga}_{1-x}\text{N}$  and  $\text{In}_y\text{Ga}_{1-y}\text{N}$  alloys", *J. Appl. Phys.* **89**, 1108 (2001).
21. S. Pezzagna, P. Vennégues, N. Grandjean, A. D. Wieck, and J. Massies, "Submicron periodic poling and chemical patterning of GaN", *Appl. Phys. Lett.* **87**, 062106 (2005).
22. M. A. Nielsen and I. L. Chuang, *Quantum Computation and Quantum Information*, (Cambridge University Press, 2000).

---

## 1. Introduction

Spontaneous parametric down-conversion (SPDC) in  $\chi^{(2)}$  nonlinear media is a well-known parametric process that allows the generation of photon pairs. In this process, the interaction of an intense pump beam with the atoms of a nonlinear medium mediates the generation of pairs of photons with lower frequency. The spatio-temporal properties of the down-converted photons depend on the specific SPDC configuration considered as well as on the spatial and temporal characteristics of the pump beam.

In most applications the goal of using SPDC is the generation of entangled photon pairs. However, the generation of photon pairs that lack any entanglement (quantum separability), but are generated in the same time window, is also of paramount importance for quantum networking and quantum information processing [1, 2, 3]. By and large, separable photon pairs are not harvested directly at the output of the down-converting crystal [4]. Their generation in a separable quantum state requires intricate control of the properties of the down-converted photons in all the degrees of freedom; namely polarization, spatial profile and frequency content. In most cases, the separability in polarization results directly from the phase matching conditions imposed by the specific SPDC configuration chosen. Separability in the spatial degree of freedom can readily be imposed by an appropriate projection of the down-converted photons into specific modes. Using single-mode fibers is one example. This leaves separability in the frequency degree of freedom as a significant challenge to achieve quantum separability between the down-converted photons.

Although one can always resort to strong spectral filtering to enhance the quantum separability of the two-photon state [5], this entails a substantial reduction in the brightness of the photon source. In the past few years, several methods have been proposed and implemented to generate frequency-uncorrelated photon pairs without the need for strong filtering. For example, elimination of the frequency correlation of photon pairs can be achieved when the operating wavelength, the nonlinear material and its length are appropriately chosen [6], as has been demonstrated in [7].

It is important to note that the appropriate conditions for the generation of frequency-uncorrelated photons might not always exist or might not be convenient for a given application [7]. The use of achromatic phase matching, or tilted-pulse techniques, allows the generation of separable two-photon states independently of the specific properties of the nonlinear medium and the wavelength used. This method employs the Poynting vector walk-off exhibited by nonlinear crystals outside noncritical phase matching to modify the effective group velocity of all the interacting waves, therefore allowing for the control of the frequency correlation [8, 9]. This is a route by which frequency-uncorrelated photons can be generated [10].

Non-collinear SPDC also allows the control of the generation of frequency-uncorrelated photons by controlling the pump-beam width and the angle of emission of the down-converted photons [11, 12]. It is indeed possible to map the spatial characteristics of the pump beam into the spectra of the generated photons (spatial-to-spectral mapping) [13], thus providing another way to manipulate the joint spectral amplitude of the biphoton, as has been demonstrated in [14]. The combination of using the pulse-tilt techniques described above together with using non-collinear geometries further expands the possibilities to control the joint spectrum of photon pairs [15]. Another approach to control the frequency correlations is to use nonlinear crystal superlattices [16].

The method presented here to generate frequency-uncorrelated photons is based on tuning the dispersive properties of the nonlinear medium itself by engineering the waveguide dispersion. The waveguide geometry allows us to enhance the source brightness and to control the dispersive properties of the propagating mode by tailoring the contribution of the waveguide dispersion to the overall dispersion. The use of Bragg reflection waveguides (BRW) based on III-V ternary semiconductor alloys ( $\text{Al}_x\text{Ga}_{1-x}\text{As}$ ,  $\text{Al}_x\text{Ga}_{1-x}\text{N}$ ) offers several advantages over conventional materials such as a large nonlinear coefficient, a broad transparency window and mature semiconductor fabrication technologies that can be utilized to tailor the spatio-temporal properties of the generated photon pairs.

Although phase-matching (PM) in these materials has often been considered as challenging due to their lack of birefringence as well as their highly dispersive nature, one can take advantage of the different dispersive properties of the various modes the waveguide can support; namely totally-internally-reflected (TIR) modes and Bragg modes. In this case, one can fully exercise a significant level of control over the dispersion properties of the interacting waves while operating at the phase-matching condition [17]. This property has been successfully used to enhance the capabilities of BRWs for generating frequency-anticorrelated photon pairs with a tunable bandwidth [18]. To even further expand the freedom of design of the dispersive properties, and thus broaden the set of possible properties of the generated photons, quasi-phase-matching, with the periodic reversal of the sign of the nonlinear coefficient  $\chi^{(2)}$ , can also be used in conjunction.

In this paper we demonstrate that Bragg reflection waveguides made of  $\text{Al}_x\text{Ga}_{1-x}\text{N}$  slabs can be tailored to generate photon pairs in a quantum separable state. Quasi-phase-matching (QPM) of the core slab is used to satisfy the phase-matching condition, while the tailoring of the dispersive properties of the waveguide, enhanced by using different types of modes for each of the interacting waves, allows us to control the frequency correlations between the down-converted photons.

## 2. Description of the quantum state of the down-converted photons

The quantum state of the down-converted photons (the signal and idler) at the output face of the waveguide, while neglecting the vacuum contribution, can be written as

$$|\Psi\rangle = \int d\Omega_s d\Omega_i \Phi(\Omega_s, \Omega_i) \hat{a}_s^\dagger(\omega_s^0 + \Omega_s) \hat{a}_i^\dagger(\omega_i^0 + \Omega_i) |0\rangle_s |0\rangle_i, \quad (1)$$

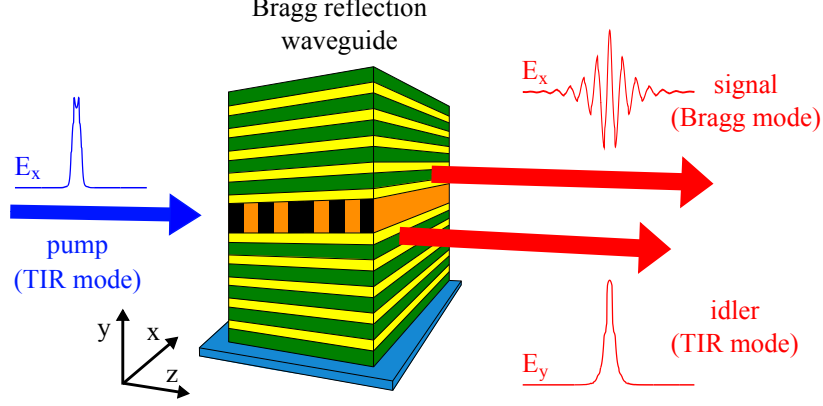


Fig. 1. General scheme for the generation of frequency-uncorrelated photon pairs. The Bragg and TIR modes have different group velocities which can be properly engineered by modifying the waveguide structure.

where  $\hat{a}_s^\dagger(\omega_s + \Omega_s)$  and  $\hat{a}_i^\dagger(\omega_i + \Omega_i)$  designate the creation operators of signal and idler photons at frequencies  $\omega_s^0 + \Omega_s$  and  $\omega_i^0 + \Omega_i$ , respectively.  $\omega_s^0 = \omega_i^0$  are the central frequencies of the signal and idler photons, and  $\Omega_{s,i}$  designate the frequency deviations from the corresponding central frequencies. The signal and idler photons are generated in specific spatial modes of the waveguide as will be described later.

The biphoton amplitude  $\Phi(\omega_s, \omega_i)$  is given by

$$\Phi(\Omega_s, \Omega_i) = \mathcal{N} E_p(\omega_s + \omega_i) \text{sinc} \left( \frac{\Delta_k L}{2} \right) \exp \left( i \frac{s_k L}{2} \right), \quad (2)$$

where  $\Delta_k = k_p - k_s - k_i$  and  $s_k = k_p + k_s + k_i$ .  $k_{p,s,i}$  are the longitudinal ( $z$ ) components of the wavevector of all the interacting photons.  $E_p$  is the spectral amplitude of the pump beam of central frequency  $\omega_p^0 = \omega_s^0 + \omega_i^0$  at the input face of the waveguide, which is assumed to be Gaussian. As such,  $E_p(\Omega_p) \sim \exp(-\Omega_p^2 / \Delta\omega_p^2)$ .  $\mathcal{N}$  is a normalizing constant, which ensures that  $\int \int d\Omega_s d\Omega_i |\Phi(\Omega_s, \Omega_i)|^2 = 1$ .

In BRWs, photons can be guided by the conventional total internal reflection (TIR modes) or by a distributed reflection from the transverse Bragg reflectors (Bragg modes). The spatial modes of the pump, signal and idler photons that we will consider here are shown schematically in Fig. 1. The pump and idler photons propagate as a TIR mode. The signal photons propagate as a Bragg mode. The use of different spatial modes for the signal and idler enhances the control of the dispersive properties of the SPDC process.

In order to get a further insight into the procedure to search for BRW configurations that generate separable paired photons, we make use of the fact that the dispersive properties of the interacting waves are different and expand their longitudinal wavevectors to first order, so that  $k_j = k_j^0 + N_j \Omega_j$  with  $j = p, s, i$ .  $k_j^{(0)}$  are the longitudinal wavevectors at the central frequencies  $\omega_j^0$ , and  $N_j$  are the inverse group velocities. Under these conditions, the biphoton amplitude can be written as

$$\begin{aligned} \Phi(\Omega_s, \Omega_i) = & \mathcal{N} \exp \left\{ -\frac{(\Omega_s + \Omega_i)^2}{\Delta\omega_p^2} \right\} \text{sinc} \left\{ [(N_p - N_s)\Omega_s + (N_p - N_i)\Omega_i] \frac{L}{2} \right\} \\ & \times \exp \left\{ i [(N_p + N_s)\Omega_s + (N_p + N_i)\Omega_i] \frac{L}{2} \right\}. \end{aligned} \quad (3)$$

Upon inspecting Eq. (3), one can show that if the inverse group velocities of the signal (idler) and pump are equal  $N_p = N_s$  ( $N_p = N_i$ ), then increasing the bandwidth of the pump beam bandwidth such that  $\Delta\omega_p \gg 1/|N_p - N_{s,i}|L$  allows us to erase all the frequency correlations between the signal and idler photons. Notice that in this case, even though there is no entanglement between the signal and idler photons, the bandwidth of one of the photons is larger than the bandwidth of the other photon. The quantum state is separable but the photons are distinguishable by their spectra.

To generate uncorrelated and indistinguishable photon pairs, the condition  $N_p = (N_s + N_i)/2$  should be fulfilled together with the condition for the bandwidth

$$\Delta\omega_p \simeq \frac{2}{\alpha L \sqrt{N_s - N_p} \sqrt{N_p - N_i}}. \quad (4)$$

This condition is obtained from approximating the sine cardinal function  $\text{sinc}(x)$  in Eq. (3) by a Gaussian function  $\exp[-(\alpha x)^2]$  with  $\alpha = 0.439$ .

To quantify the degree of entanglement of the generated two-photon state, we calculate the Schmidt decomposition of the biphoton amplitude, i.e.,  $\Phi(\Omega_s, \Omega_i) = \sum_{n=0}^{\infty} \sqrt{\lambda_n} U_n(\Omega_s) V_n(\Omega_i)$ , where  $\lambda_n$  are the Schmidt eigenvalues and  $U_n$  and  $V_n$  are the corresponding Schmidt modes. The degree of entanglement of the two-photon state can be quantified by means of the purity of either of the subsystems (signal or idler photons) that make up the whole system. The purity of either subsystem is given by  $P = K^{-1}$ , where  $K = \sum_{n=0}^{\infty} \lambda_n$ .  $K = 1$  corresponds to a separable two-photon state, while an increasing value of  $K$  corresponds to an increase in the degree of entanglement.

### 3. Design of BRW structures to generate uncorrelated photon pairs

Let us consider the generation of paired photons in the C-band of the optical communication window, i.e., let the central wavelength of both emitted photons be 1550 nm. Therefore, for the frequency-degenerate case, the central wavelength of the pump beam is 775 nm. The main parameters that characterize the dispersion properties of the Bragg modes, and that can be

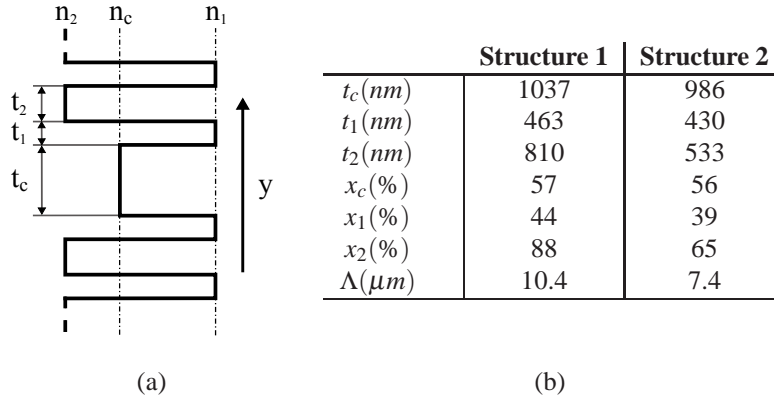


Fig. 2. (a) Profile of the refractive index along the y-axis of the Bragg reflection waveguide.  $t_c$  - core thickness;  $t_{1,2}$  - thicknesses of the alternating layers of the Bragg reflector;  $x_c$  - aluminium concentration in the core;  $x_{1,2}$  - aluminium concentration in the reflector's layers;  $\Lambda$  - quasi-phase-matching period. Both structures are 4 mm long and they are optimized for type-II SPDC.

engineered to tailor the spectral properties of the down-converted photons, are the thickness of the layers and their aluminium fraction.

BRW structures for the generation of frequency-uncorrelated photon pairs were obtained by numerically solving the Maxwell equations inside the waveguide using the finite element method [19]. Since many solutions were found, a genetic algorithm was used to select waveguides with the properties that are most suitable for practical implementation. The thicknesses and the corresponding aluminum fractions of two of the structures obtained are given in Fig. 2.

The refractive indices for the calculations were taken from [20]. The Bragg reflection waveguides are composed of 12 bi-layers above and below the core. Both structures were optimized for the Bragg mode propagation at the quarter-wave condition for the central wavelength, which maximizes the energy confinement in the core.

Type-II SPDC interactions are considered for both structures, even though structures with type-I or type-0 interactions can also be designed. One of the advantages of type-II phase-matching is that the generated photons can easily be separated at the output of the waveguide. The pump and signal photons have TE polarization and the idler photons have TM polarization. The signal photons propagate as a Bragg mode, whereas the idler photons propagate as a TIR mode. The quasi-phase-matching can be achieved, for example, by the method described in [21]. The quasi-phase-matching periods  $\Lambda$  were calculated from the phase-matching condition  $\Delta_k - \frac{2\pi}{\Lambda} = 0$ , where  $\Delta_k$  is the phase-mismatch function at the central frequencies of all interacting waves.

The spatial overlap between the modes of the interacting photons is defined as

$$\Gamma = \int dx u_p(x) u_s^*(x) u_i^*(x), \quad (5)$$

where  $u_j(x)$   $j = p, s, i$  are the mode functions describing the transverse distribution of the electric field in the waveguide. The overlap reaches 40.5% for Structure 1 and 19.4% for Structure 2. The combination of the high effective nonlinear coefficient and the overlap results in an efficiency that is still much higher than with other phase-matching platforms in waveguides or bulk media. Although the thickness of the core of both structures is sufficiently large so that higher-order modes (both TIR and Bragg modes) could exist, they lack phase-matching and their overlap is very small.

### 3.1. Uncorrelated photon pairs with different spectra

Structure 1 provides a configuration to generate a quantum separable state with different spectral bandwidths of the signal and idler photons. The group velocities of the pump and signal photons are equal. We find that  $v_p = v_s = 0.445c$ , where  $c$  is the speed of light in a vacuum.

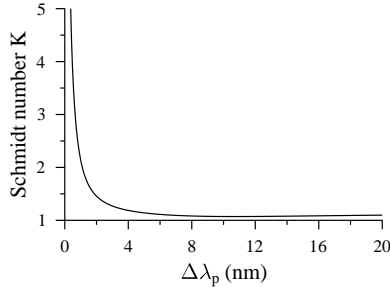


Fig. 3. The Schmidt number K as a function of the bandwidth of the pump beam  $\Delta\lambda_p$ .

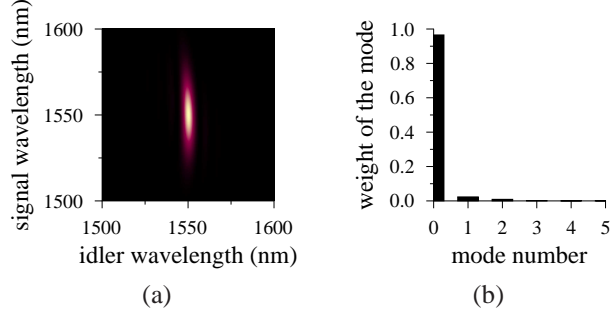


Fig. 4. (a) Joint spectral intensity of the biphoton generated in Structure 1 for  $\Delta\lambda_p=10$  nm. (b) The Schmidt decomposition corresponding to this quantum state.

The dependency of the Schmidt number  $K$  on the pump beam bandwidth is plotted in Fig. 3. A highly separable quantum state can be obtained for a pump beam bandwidth  $\Delta\lambda_p \geq 10$  nm. For values of  $\Delta\lambda_p < 1$  nm, the paired photons turn out to be anti-correlated.

The joint spectral intensity of the biphoton is showed in Fig. 4(a). It shows a cigar-like shape oriented along the signal wavelength axis, as expected from the fulfillment of the condition  $N_p = N_s$ . The Schmidt decomposition is shown in Fig. 4(b). Clearly, this decomposition corresponds to a nearly ideal case of frequency-uncorrelated photons. For the case shown in Fig. 4, with a pump beam bandwidth (FWHM) of 10 nm, the bandwidths of the signal and idler photons are 47.5 nm and 8 nm, respectively. The entropy of entanglement is used as a measure of spectral correlation [22] and is defined as  $E = -\sum_i \lambda_i \log_2 \lambda_i$ . The obtained value is 0.257 in this case.

### 3.2. Uncorrelated photon pairs with identical spectra

Structure 2 is designed for the generation of a separable two-photon state where both photons exhibit the same spectra. The calculated values of the group velocities of all the waves are  $v_p = 0.44c$ ,  $v_s = 0.4252c$  and  $v_i = 0.456c$ . Figure 5 shows the value of the Schmidt number  $K$  as a function of the pump beam bandwidth. The optimum pump bandwidth for the generation of frequency-uncorrelated photons is found to be  $\Delta\lambda_p = 1.3$  nm, for which  $K$  achieves its lowest value. The value of  $K$  cannot reach the ideal value of 1 due to the presence of the side-lobes of the sinc function in the anti-diagonal direction and a Gaussian profile in the diagonal direction that introduces a slight asymmetry (see Eq. 3). Figure 6(a) shows the joint spectral intensity

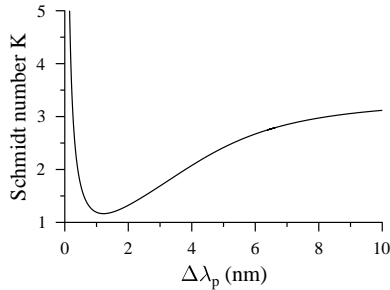


Fig. 5. The Schmidt number  $K$  of the state generated in Structure 2 as a function of pump bandwidth  $\Delta\lambda_p$ .



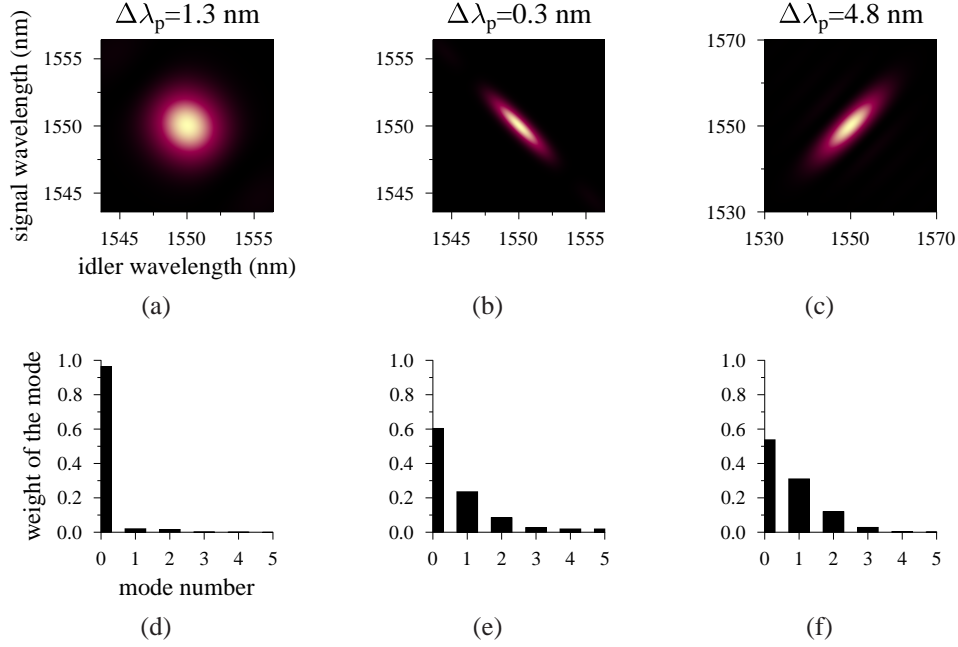


Fig. 6. Joint spectral intensity of photons generated in Structure 2 for different pump bandwidths: a)  $\Delta\lambda_p = 1.3$  nm, b)  $\Delta\lambda_p = 0.3$  nm and c)  $\Delta\lambda_p = 4.8$  nm. Plots (d), (e) and (f) in the second line are the corresponding Schmidt decompositions.

of frequency-uncorrelated photons, when this optimum value of the pump bandwidth is used. Figure 6(d) shows the corresponding Schmidt decomposition. The entropy of entanglement is 0.267 and the bandwidth is 4.5 nm for both signal and idler photons.

For smaller values of the pump beam bandwidth, the photons generated in Structure 2 correspond to photon pairs that are anticorrelated in frequency (see Fig. 6(b)), whereas the use of larger values allows the generation of frequency-correlated photon pairs (see Fig. 6(c)). Figures 6(e) and (f) show the Schmidt decompositions corresponding to each of these cases.

#### 4. Conclusion

We have presented and analyzed a new source for photon pairs that allows the generation of paired photons that lack any frequency correlation. These are of paramount importance for quantum networking technologies and quantum information processing. The source is based on Bragg reflection waveguides composed of  $\text{Al}_x\text{Ga}_{1-x}\text{N}$ . Quasi-phase-matching of the waveguide core is used to achieve phase-matching at the desired wavelength. The control of BRW dispersion is used to control the frequency correlation between the generated photons.

Two Bragg reflection waveguide structures have been presented. One of the structures allows us to generate uncorrelated photons with different spectra. The down-converted uncorrelated photons generated in the second structure are spectrally indistinguishable.

This technique offers a promising route for the realization of electrically pumped, monolithic photon-pair sources on a chip with versatile characteristics.



## **5. Acknowledgments**

This work was supported by the Government of Spain (Consolider Ingenio CSD2006-00019, FIS2010-14831). This work was also supported in part by FONCICYT project 94142 and by projects IAA100100713 of GA AVČR, COST OC 09026.